BULLETIN OF THE POLISH ACADEMY OF SCIENCES
TECHNICAL SCIENCES, Vol. 73(4), 2025, Article number: e153437
DOI: 10.24425/bpasts.2025.153437



# Three-axis forces and torque sensor

**Paweł MŁOTEK, Piotr MYNAREK, and Marcin KOWOL***

Faculty of Electrical Engineering, Automatic Control and Informatics, Opole University of Technology, Opole, Poland

**Abstract.** This paper describes research on a prototype of a multi-axis force and torque sensor dedicated to the support system of a telescopic camera crane arm. Based on studies conducted on an actual telescopic camera crane arm, the requirements that the sensor must meet to enable precise control of the drives in two working axes of the telescopic camera crane arm were defined. In the sensor developed, a method for measuring forces and torques using an optical displacement sensor was proposed. A simplified sensor prototype was made to verify the assumptions, and measurement tests were carried out. Additionally, the paper presents a CAD model of the sensor using an elastic pin, based on which a numerical model was developed, and calculations of displacements and mechanical stresses were performed.

**Keywords:** three-axis force and torque sensor; optical measurement of force and torque; STM microcontroller; structural analysis.

## 1. INTRODUCTION

In today's rapidly developing science and technology, force and torque sensors have become indispensable. They serve as elements for precise measurement in various industrial applications related to drive technology, robotics, biomechanics, and advanced user interfaces. Force sensors are built based on different physical phenomena and differ in operating principles [1]. Currently, strain gauge sensors are commonly used to utilize changes in material resistance under mechanical stress. They are mounted onto various structural elements, and the changes in resistance are measured and converted/scaled to force values [2]. These sensors require calibration and temperature compensation, and their chief disadvantage lies in their sensitivity to electromagnetic interference and damage caused by water ingress into the sensor [1].

Piezoelectric sensors are based on the piezoelectric effect, where a crystal generates electric charges in response to mechanical stress. They are characterized by high sensitivity to dynamic force changes. Capacitive sensors use changes in capacitance between electrodes caused by material deformation and are often used in micromachines and applications requiring high sensitivity.

A completely separate group, highly diverse in implementation, are optical force sensors that use optical phenomena for force measurement. Interferometric sensors are based on light interference, where a change in the optical path length due to mechanical forces leads to a change in interference, which is then measured. Fiber optic sensors use optical fibers as the measuring element, where mechanical deformation changes the parameters of the light passing through the fiber, allowing for force measurement. Another group of force sensors includes sensors that utilize changes in optical parameters, such as lens focal length, under mechanical forces. These changes are measured and analyzed to determine the force value [2–4].

This paper presents an innovative approach using an optical displacement sensor to measure relatively large forces and torque acting on a telescopic camera crane arm during its operation (Fig. 1). A precise and inexpensive multi-axis force and torque sensor opens up new possibilities in the field of continuous, accurate tracking of the operator's movements controlling the crane. The new measurement transducer also opens up the possibility of adaptive control of the electric drive system, assisting the movement of such a device to improve work safety and ergonomics.

**Fig. 1.** MB45 telescopic camera crane arm in operation

## 2. REQUIREMENTS FOR THE TELESCOPIC CAMERA CRANE ARM MOTION ASSIST SYSTEM

Telescopic camera jibs are devices used in the film and television industry to lift the camera recording the image, which is installed at the end of its arm. The sizes of the jibs reach up to twenty meters in length, and their total weight can reach up to three tons. These devices are currently operated solely by one person's muscle power. It is easy to imagine that the skills of

*e-mail: M.Kowol@po.edu.pl

Manuscript submitted 2024-09-02, revised 2024-12-03, initially accepted for publication 2025-01-23, published in July 2025.

the crane operator are closely related to their physical strength. Even at low angular velocities of the arm, in its working axes PAN (horizontal axis) and TILT (vertical axis), the moments of inertia of the entire system reach even 32 717 $m^2$·kg. In the first stage of research on the prototype of the electric motion assist system for the largest jibs of the MB50XL type, a series of measurements of mechanical quantities were conducted using a proprietary data acquisition system. Detailed results were presented in [5]. From the measurements, the limit value of the force exerted by the operator on the rear handle of the jib was obtained, which is 800 N. Similarly, the torque exerted on the handle mounting system can reach up to 300 N·m in an extreme case. After analyzing the work cycle of the telescopic camera jib, it was found that the sensor to be designed should be a system with at least three degrees of freedom, allowing for the measurement of linear forces in two axes and torque. Additionally, the following requirements for the force and torque sensor, enabling proper control of the motion assist drive system, were defined:

- Measurement range of forces: ±900 N;
- Measurement range of torque: ±300 N·m;
- High resolution, ensuring adequate system sensitivity;
- Data refresh rate of the measurement system at 100 Hz;
- Repeatability of the read position at the level of 98%;
- No drift of the read position at rest;
- Digital output of the measured parameters;
- Measurement stability in the range of 0–40°C;
- Self-diagnosis.

## 3. PROTOTYPE OF THE OPTICAL FORCE AND TORQUE SENSOR

The PixArt PMW3360 optical sensor, widely used in high-end computer mice, was utilized to build a three-axis force and torque sensor. This system is characterized by high resolution, amounting to 12000 CPI, which is extremely important in the application being discussed. The basic technical parameters of the system are presented in Table 1.

**Table 1**
Technical parameters of the PMW3360 optical sensor

| Parameter | Value | Unit |
|---|---|---|
| Lens | 1:1 | – |
| Interface | SPI | – |
| System clock | 70 | MHz |
| Refresh rate | 12 000 | fps |
| Resolution | 12 000 | cpi |
| Resolution error | 1 | % |
| Operating temperature | 0–40 | °C |

In the initial research phase, a single-axis sensor system was built according to the schematic illustrated in Fig. 2. Based on the system constructed, accuracy and repeatability tests were conducted for various reflective surfaces.

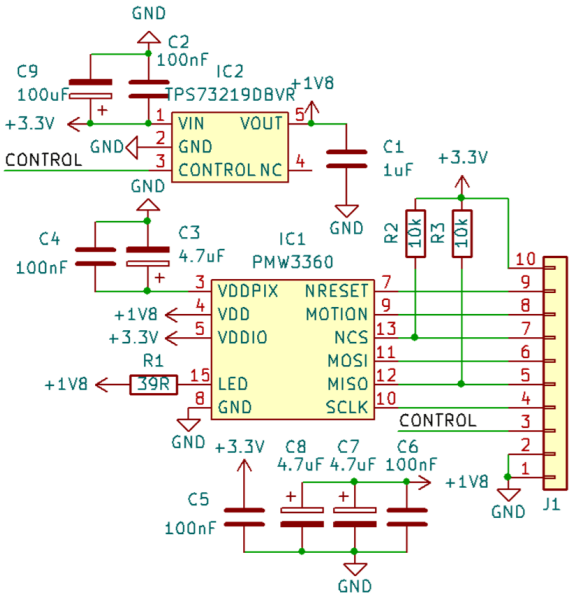


**Fig. 2.** Schematic of PMW3360 sensor connections

A Fanuc LR Mate 200iC robot was used to conduct the accuracy and repeatability tests. A sensor system, prepared earlier, was mounted onto the robot's end effector (Fig. 3). A 3DConnexion pad, ensuring surface uniformity throughout the movement area, was used as the substrate. An STM32 microcontroller-based platform was used to process the data collected from the sensor.

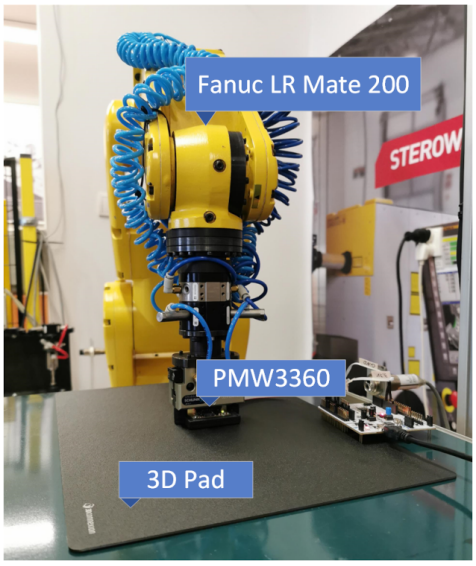


**Fig. 3.** Test stand for the optical sensor

In the first stage of the tests, the robot arm moved separately in the X and Y axes, with a movement range of ±10 mm relative to the start/reference point in each axis. Data obtained directly from the sensor monitoring the movement are shown in Fig. 4 (range around 9500 CPI). It can be observed that despite the one-axis movement trajectory of the arm, the sensor also registered a slight change in position in the direction perpendicular to the

set axis. The change detected in the position in the axis perpendicular to the movement is at a marginal level (about 20 times lower). This is partly caused by the non-orthogonal mounting of the sensor relative to the robot's coordinate system. The recorded characteristics during five repetitions of measurements for the set trajectory in the X and Y axes (Fig. 4a and 4b, respectively) do not overlap. The discrepancies between the characteristics result from the very high sensitivity of the sensor but successfully meet the criteria set in the assumptions. As with any measurement system, calibration always plays an important role. The measurements showed that it is possible to accurately determine the correction coefficient during the sensor calibration stage, effectively eliminating difficult-to-avoid assembly errors/tolerances. Noticeable position deformations may result from the sensor mounting position and minimal play in the robot's joints when changing movement direction.

In the next research phase, position errors were checked during movement in all directions. For this purpose, a series of robot movements along a circular trajectory with a diameter of 40 mm was performed (Fig. 5). Analyzing the results obtained, it can be stated that the starting and initial positions read from the sensor practically overlap. In this case as well, the return of the position to the starting point proves the precision of the PMW3360 sensor.

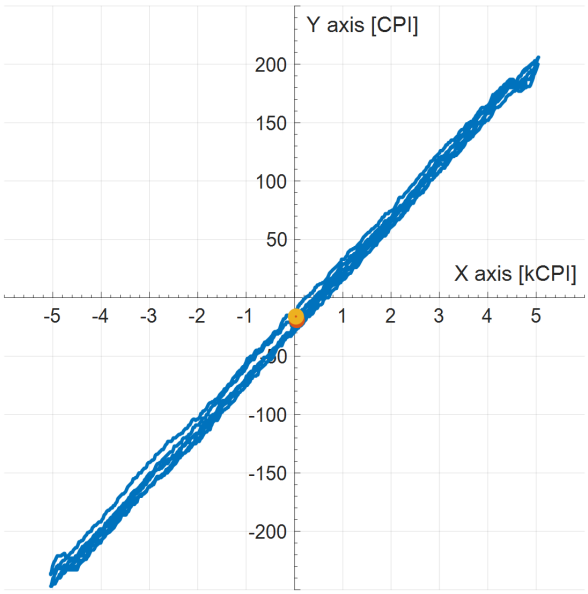


(a)

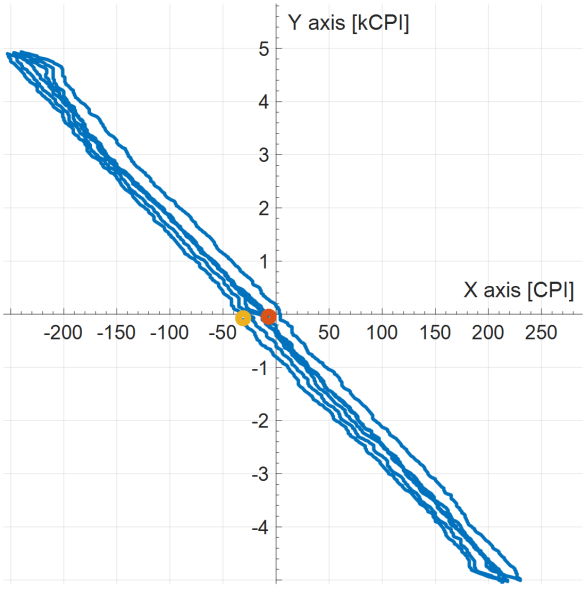


(b)

**Fig. 4.** Cyclic movement of the sensor in the axis: (a) X and (b) Y

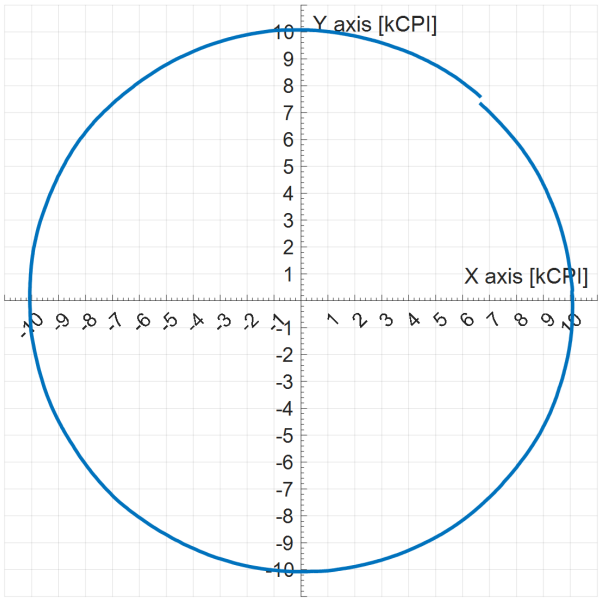


**Fig. 5.** Example of sensor movement along a circle with a diameter of 40 mm

Another important parameter is the resting position drift. However, this phenomenon was not detected during the several-hour tests conducted. In the resting state, the measured position remains unchanged. Assuming high repeatability of the robot arm position, it can be concluded that the position error returned by the proposed sensor is repeatable and does not exceed 2%. The results confirm the possibility of using the PMW3360 optical system to build a multi-axis force and torque sensor.

## 4. CONSTRUCTION MODEL OF THE SENSOR

Having tested the PMW3360 optical system, we designed a three-axis force and torque sensor. The sensor concept is based on two PMW3360 sensors installed on the X-axis but with a reversed orientation (Fig. 6).

The entire assembly is attached via a coupling to an elastic element, which connects the back of the jib and the operator's handle (Fig. 7). The use of two sensors allows for easy detection of torque and its direction exerted on the elastic element.

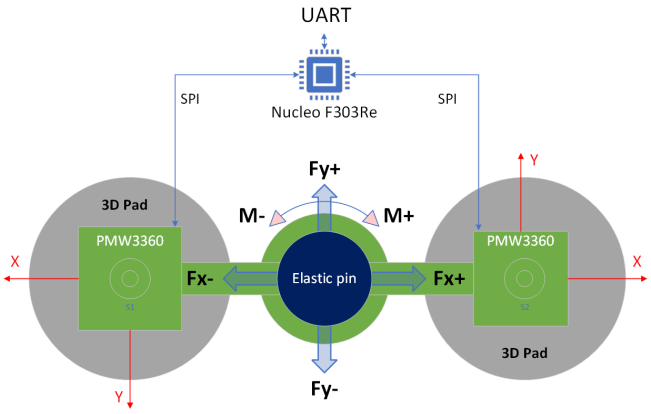


**Fig. 6.** Three-axis sensor – block diagram

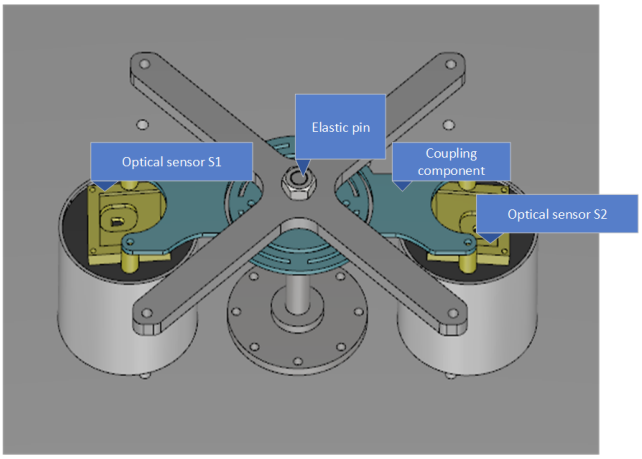


**Fig. 7.** Three-axis sensor – construction model

## 5. STRENGTH CALCULATIONS FOR THE ELASTIC ELEMENT OF THE SENSOR

The validity and effectiveness of the proposed prototype of the three-axis force and torque sensor depend on the correct selection of the elastic element shown in Fig. 7. This element serves as a pin-shaped connector between the back of the boom arm and the operator's handle. The pin should also exhibit elasticity that, within the defined ranges of force ($F = \pm 800$ N) and torque ($T = \pm 300$ N·m), allows for precise measurement using the PMW3360 optical sensor. Therefore, it was decided to manufacture this element from S960QL steel, whose physical parameters are presented in Table 2.

**Table 2**
Physical parameters of S960QL steel [7]

| | | |
|---|---|---|
| Young's modulus – $E$ | [MPa] | $2.2 \cdot 10^5$ |
| Yield strength – $R_{p0,2}$ | [MPa] | 974 |
| Tensile strength – $R_m$ | [MPa] | 1070 |
| Shear modulus – $G$ | [MPa] | $8 \cdot 10^4$ |
| Percentage elongation after a fracture – $A$ | [%] | 14.2 |
| Percentage reduction of area – $Z$ | [%] | 45.6 |

While conducting a strength analysis of the discussed pin, it can be treated as a cantilever beam that undergoes deflection and stress during operator use. According to Euler-Bernoulli beam theory, the displacement of the pin can be determined using the following formula [8]:

$$\delta = \frac{F \cdot L^3}{3 \cdot E \cdot I}, \tag{1}$$

where: $\delta$ – maximum deflection of the beam (at the point of force application), $F$ – force applied, $L$ – beam length, $E$ – Young's modulus of the material, $I$ – moment of inertia of the beam's cross-section relative to the bending axis – $6.622 \cdot 10^{-9}$ m$^4$.

For the analyzed case, with a force $F = 800$ N applied to the pin, the deflection is $\delta = 3.21$ mm. According to the Saint-Venant torsion theory, expressed by (2), the presence of torque in the system does not affect the displacement of the pin.

Torsion only results in the rotation of the cross-section. In the case being analyzed, with maximum torque of $T = 300$ N·m applied to the pin, the twist angle is $\varphi = 5.3°$

$$\varphi = \frac{T \cdot L}{G \cdot J}, \tag{2}$$

where $T$ – torque applied, $L$ – beam length, $G$ – shear modulus of the material.

A numerical model of the pin was also developed to verify the results. Using the finite element method, a strength analysis was conducted. Figure 8 shows the results of two simulations of the pin displacement being analyzed. In the first case, the pin is subjected only to a force along the X-axis of 800 N (Fig. 8a). In the second case, additional torque of 300 N·m is applied (Fig. 8b). Maximum displacements obtained in both cases are 3.21 mm. The presence of additional torque does not increase the displacement of the pin, which confirms the Saint-Venant torsion theory [8].

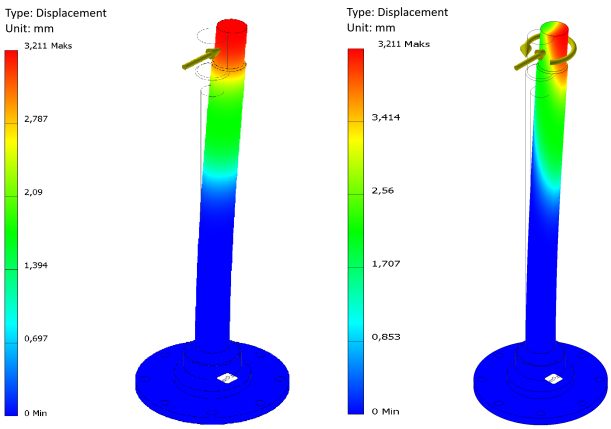


(a) (b)

**Fig. 8.** Displacement simulation of the pin for (a) force of 800 N, (b) force of 800 N and torque of 300 N·m

With an accuracy of up to three-thousandths of a millimeter, the difference between the analytical and numerical calculations is negligible.

Accuracy of the discussed sensor prototype's operation is influenced by the variability of the pin's displacement ($\delta$) under the forces applied ($F$). Based on (1), it can be stated that the relationship between force and pin displacement is linear. This information is crucial for accurately determining the torque the assistance system should exert.

In the next step, calculations were conducted to determine the stresses occurring in the pin under extreme operating conditions. Figure 9 illustrates the stresses acting on the pin for the cases considered in this study. Maximum stress in the pin under a force of 800 N applied to the system is 441 MPa, while with the additional torque of 300 N·m, the stress increases to approximately 783 MPa.

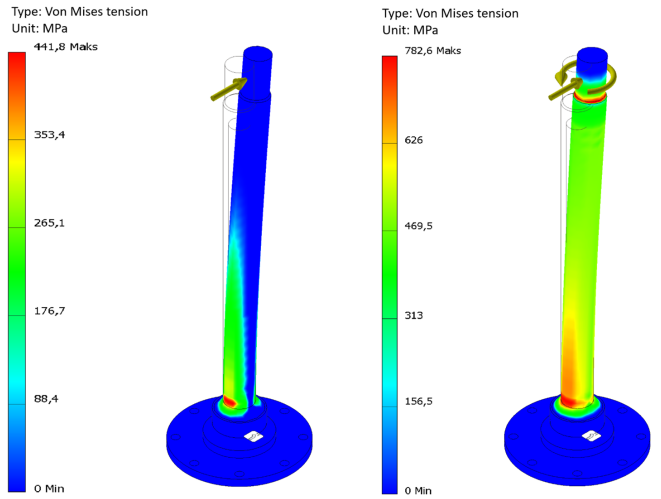


(a) (b)

**Fig. 9.** Pin stress simulation for (a) force of 800 N, (b) force of 800 N and torque of 300 N·m

As per the widely used Huber-Mises hypothesis [6], the stress results obtained do not pose a risk of failure for the elastic pin. Based on this hypothesis, it is assumed that the material fails when the von Mises equivalent stress (3) exceeds the critical value, meaning the material reaches its yield strength, beyond which it undergoes permanent deformation.

$$\sigma_{vm} = \sqrt{\frac{1}{2}\left[(\sigma_1-\sigma_2)^2+(\sigma_2-\sigma_3)^2+(\sigma_3-\sigma_1)^2\right]}, \qquad (3)$$

where $\sigma_{vm}$ – von Mises equivalent stress $\sigma_1$, $\sigma_2$, $\sigma_3$ – principal stresses (components of the stress state along the principal axes).

For the pin under discussion, the yield strength is 974 MPa, which is approximately 190 MPa higher than the stress at the maximum values of force and torque acting on the boom. The safety factor (4) calculated for the tested object is $n = 1.24$.

$$n = \frac{R_{0.2}}{\sigma}, \qquad (4)$$

where $R_{p0.2}$ – stress defining the yield strength of the material, $\sigma$ – stress present in the system.

In the case being discussed, to reach the yield strength, it would be necessary to:

- apply a force of 2100 N or torque of 510 N·m,
- apply a force of 800 N along with torque of 470 N·m,
- apply torque of 300 N·m and a force of 1700 N.

## 6. SENSOR CALIBRATION

During the tests conducted on the sensor prototype, it was observed that the results were affected by errors caused by the non-orthogonality of the PMW3360 sensors' positions resulting from the assembly process (Fig. 10). To eliminate these errors, calibration is necessary to determine the non-orthogonality angles for all axes of the sensor. The calibration process must be performed independently for both sensors.

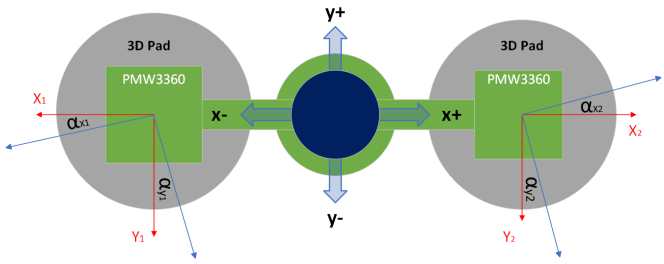


**Fig. 10.** Diagram of the sensor with marked non-orthogonality angles

The calibration process involved mounting the sensor prototype onto the end effector of a Fanuc LR Mate 200 robot using coupling, and performing movements along individual axes. Based on the data collected by the acquisition system, the non-orthogonality angles for both sensors' X and Y axes were determined.

**Fig. 11.** Calibration process using the Fanuc LR Mate 200 robot

With the determined values of the non-orthogonality angles for all axes, it is possible to calculate the corrections needed for the sensor measurements to obtain accurate displacement values (5) and (6).

$$F_x = \tan\alpha_x \cdot y, \qquad (5)$$

$$F_y = \tan\alpha_y \cdot x, \qquad (6)$$

where $F_x$, $F_y$ – correction factor for the X-axis, Y-axis, $\alpha_x$, $\alpha_y$ – non-orthogonality angle in the X-axis, Y-axis, $x$, $y$ – displacement in the X-axis, Y-axis.

After introducing corrections resulting from non-orthogonality and based on relationships (1) and (2), it is possible to determine the force (7) and torque (8) acting on the analyzed pin. The force and torque can be considered independently using a linear equation, significantly simplifying further control of the boom support system.

$$F = \frac{3\delta \cdot E \cdot I}{L^3}, \tag{7}$$

where $\delta$ – for the sensor applied, is described by the following relationship: number of pulses $2.12 \cdot 10^{-6}$ m

$$T = \frac{\varphi \cdot G \cdot J}{L}, \tag{8}$$

where $\varphi$ – the twist angle of the pin, whose $\tan(\varphi) = \Delta Y / D$, $D$ – distance from the sensor to the center of the pin, expressed in sensor pulses = 48 349 pulses. $\Delta Y$ – displacement resulting from torsion, expressed in sensor pulses.

## 7. SUMMARY

The article presents an innovative use of an optical displacement sensor to measure the forces and torques exerted by the operator of a camera jib on its handle. It should be noted that currently no sensors available in the market could be applied to the jib presented in this study. The prototype uses the PixArt PMW3360 sensor, characterized by high resolution and stability. Tests have shown that the sensor's measurement error does not exceed 2%, and the lack of position drift at rest confirms its reliability. The three-dimensional numerical model and finite element calculations confirmed that the displacements are within the measurement range, making this system a promising solution for precisely monitoring telescopic camera jibs.

## REFERENCES

[1] J.O. Templeman, B.B. Sheil, and T. Sun, "Multi-axis force sensors: A state-of-the-art review," *Sens. Actuators A-Phys.*, vol. 304, p. 111772, Apr. 2020, doi: 10.1016/j.sna.2019.111772.

[2] V. Grosu, S. Grosu, B. Vanderborght, D. Lefeber, and C. Rodriguez-Guerrero, "Multi-axis force sensor for human-robot interaction sensing in a rehabilitation robotic device," *Sensors (Switzerland)*, vol. 17, no. 6, p. 1294, 2017, doi: 10.3390/s17061294.

[3] J.-H. Kim, "Multi-Axis Force-Torque Sensors for Measuring Zero-Moment Point in Humanoid Robots: A Review," *IEEE Sens. J.*, vol. 20, no. 3, pp. 1126–1141, Feb. 2020, doi: 10.1109/JSEN.2019.2947719.

[4] Y. Noh *et al.*, "Multi-Axis Force/Torque Sensor Based on Simply Supported Beam and Optoelectronics," *Sensors*, vol. 16, no. 11, p. 1936, Nov. 2016, doi: 10.3390/s16111936.

[5] P. Młotek, P. Warmuzek, M. Łukaniszyn, M. Kowol, J. Kołodziej, and P. Mynarek, "Wyznaczanie parametrów elektromechanicznych napędu wspomagającego pracę teleskopowych wysięgników do kamer", XLV *Konferencja z Podstaw Elektrotechniki i Teorii Obwodów SPETO*, 2024. (in Polish)

[6] T. Niezgodziński and E Michał, *Wytrzymałość materiałów*. Warszawa: Wydawnictwo Naukowe PWN, 2010.

[7] T. Ślęzak and L. Śnieżek, "A comparative LCF study of S960QL high strength steel and S355J2 mild steel", *Procedia Eng.*, vol. 114, pp. 78–85, 2015.

[8] S. Timoshenko, *History of strength of materials*. Italy: Dover Publications, 1983, pp. 135–141.